

$\gamma^{(*)}\gamma^{(*)}$ reactions at high energies[‡]

A Donnachie[†] and S Söldner-Rembold[‡]

[†] Department of Physics, Manchester University, UK, ad@a13.ph.man.ac.uk

[‡] CERN, Geneva, Switzerland, stefan.soldner-rembold@cern.ch

Abstract. The energy available for $\gamma^{(*)}\gamma^{(*)}$ physics at LEP2 is opening a new window on the study of diffractive phenomena, both non-perturbative and perturbative. We discuss some of the uncertainties and problems connected with the experimental measurements and their interpretation.

1. Introduction

Diffractive phenomena occur in each of untagged, single-tagged and double-tagged photon-photon reactions via the total hadronic $\gamma\gamma$ cross-section, $\sigma_{\gamma\gamma}$; the structure function of the real photon, F_2^γ (or equivalently the $\gamma^*\gamma$ cross-section); and the total hadronic $\gamma^*\gamma^*$ cross-section, $\sigma_{\gamma^*\gamma^*}$ respectively. Thus in principle it is possible to study diffraction continuously from the quasi-hadronic regime dominated by non-perturbative physics to the realm of perturbative QCD with either single or double hard scales.

2. $\gamma\gamma$ scattering

The total hadronic $\gamma\gamma$ cross-section was measured at LEP in the ranges $5 \leq W \leq 145$ GeV [1, 2] and $10 \leq W \leq 110$ GeV [3], where W is the photon-photon centre-of-mass energy (Fig. 1). Since the use of different Monte Carlo models (PYTHIA [4]

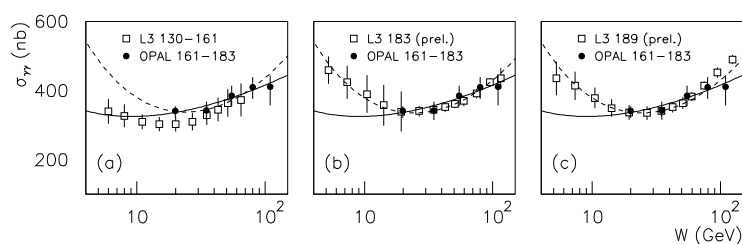


Figure 1. OPAL data at $\sqrt{s_{ee}} = 161 - 183$ GeV in comparison to the L3 data at $\sqrt{s_{ee}} = 130 - 161$ GeV (a), at $\sqrt{s_{ee}} = 183$ GeV (b) and at $\sqrt{s_{ee}} = 189$ GeV (c). In all cases PHOJET was used for the unfolding of detector effects. The continuous line is a fit to the OPAL data, the dashed line a fit to the L3 data at $\sqrt{s_{ee}} = 183 - 189$ GeV (see text).

or PHOJET [5]) for the unfolding of detector effects leads to significant shifts of the

[‡] submitted to proceedings of the Durham Collider Workshop, Durham, UK, 22-26 September 1999

normalisation, the results of the two experiments are compared using only PHOJET for these corrections[§].

Both experiments have measured the high energy rise of the total cross-section typical for hadronic interactions. However a faster rise of the total $\gamma\gamma$ cross-section with W compared to purely hadronic interactions has not been unambiguously observed. This faster rise is predicted by most models for $\gamma\gamma$ interactions.

To quantify this effect, both experiments have fitted a Donnachie-Landshoff parametrisation of the form $\sigma_{\gamma\gamma} = Xs^\epsilon + Ys^{-\eta}$ with $\eta = 0.34$. The results are $\epsilon = 0.10 \pm 0.02$ (OPAL) and $\epsilon = 0.22 \pm 0.02$ (L3), where the L3 fit uses only the preliminary data at $\sqrt{s_{ee}} = 183 - 189$ GeV. The fitted curves are also shown in Fig. 1. The L3 result implies a significantly faster rise of the total $\gamma\gamma$ cross-section than in hadron-hadron scattering whereas the OPAL result is consistent with a typical value of $\epsilon \approx 0.08$ for a soft Pomeron.

The results are consistent in the kinematic region where the measurements of both experiments overlap. Some discrepancies seem to exist between the L3 measurements at different $\sqrt{s_{ee}}$, both at low and at high W . The data in the range $W < 10$ GeV also have large influence on the fitted value of ϵ due to the large correlation between the Reggeon-Term Y and ϵ .

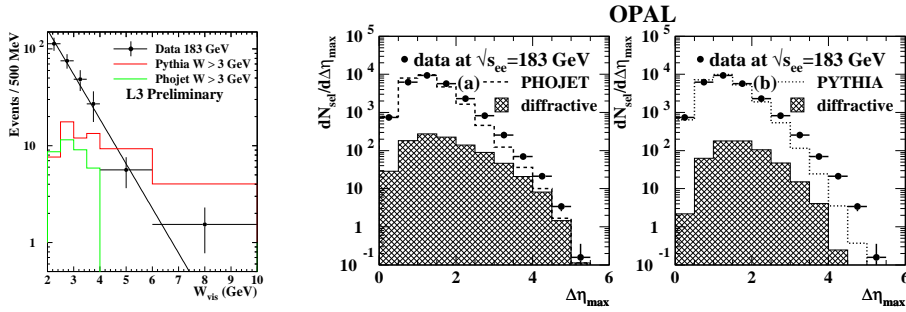


Figure 2. Left plot (L3): number of $\gamma\gamma \rightarrow \rho^0 X$ events as a function of the visible W (W_{vis}). Right plots (OPAL): number of selected two-photon events in the range $6 < W_{\text{vis}} < 120$ GeV as a function of the maximum rapidity gap, $\Delta\eta_{\text{max}}$, between any two particles (tracks and calorimeter clusters). For the MC, the diffractive events (including quasi-elastic scattering) are shown separately.

The main problems of this measurement are the resolution effects in the reconstruction of W from the hadronic final state and the small acceptance for events coming from soft diffractive or quasi-elastic processes (e.g. $\gamma\gamma \rightarrow \rho\rho$) which lead to the large model dependence for the final results. The W resolution makes it necessary to use unfolding models which introduce large bin-to-bin correlations. The acceptance for soft diffractive and quasi-elastic processes is only 5-15%, depending on the W range and on the MC model used [3]. For $W > 20$ GeV the average polar angle of the pions in $\gamma\gamma \rightarrow \rho\rho$ events is less than 100 mrad, well below the tracking coverage of the LEP detectors. L3 has therefore measured inclusive ρ production in $\gamma\gamma$ events for $3 \leq W \leq 10$ GeV. In this W region large discrepancies between the Monte Carlo models and the data are observed (Fig. 2). At higher W OPAL has studied the maximum rapidity gap $\Delta\eta_{\text{max}}$ between any two particles (tracks and

[§] The published OPAL data are given after averaging the PHOJET and the PYTHIA corrected results (Fig. 3).

calorimeter clusters) in an event. At high $\Delta\eta_{\max}$, where diffractive events are expected to contribute, the data lie above the Monte Carlo models and PHOJET is closer to the data than PYTHIA.

Soft processes like quasi-elastic scattering ($\gamma\gamma \rightarrow VV$, where V is a vector meson), single-diffractive scattering ($\gamma\gamma \rightarrow VX$, where X is a low mass hadronic system) or double-diffractive scattering ($\gamma\gamma \rightarrow X_1X_2$) are modelled by both generators. The cross-sections are obtained by fitting a Regge parametrisation to pp, $p\bar{p}$ and γp data and by assuming Regge factorisation, i.e. universal couplings of the Pomeron to the hadronic fluctuations of the photon. In both generators the quasi-elastic cross-section is about 5 – 6%, the single-diffractive cross-section about 8 – 12% and the double-diffractive cross-section about 3 – 4% of $\sigma_{\gamma\gamma}$ for $W > 10$ GeV. In the $\gamma\gamma$ data no clear diffractive signal has yet been observed and it would be very useful to find experimental variables which could give a better discrimination between diffractive and non-diffractive events at LEP and which could be used to test the Monte Carlo models.

3. The hard Pomeron model and the dipole formalism

As the energies and virtualities available at LEP are comparatively moderate it is necessary to take into account diffractive and non-diffractive contributions. There are two main sources of the non-diffractive contributions: Reggeon exchange and the quark box diagram with pointlike couplings of the photon. In Regge language the latter gives rise to a fixed pole in the complex angular momentum plane, so it is not dual to Regge exchange and it is correct to add the two contributions. The box diagram is well defined [6]. The Regge contribution to F_2^γ can be estimated [7] using the DGLAP evolved pion structure function and naive VMD. This can be extended to both the $\gamma\gamma$ and $\gamma^*\gamma^*$ cross-sections assuming factorization [8]. In the dipole approach to the small- x structure function of the proton it has become increasingly clear that the nominally perturbative regime still contains some non-perturbative contribution [9, 10, 11]. A specific model has been proposed in terms of two Pomerons [12, 13, 14]. This combines a hard Pomeron with an intercept of about 1.44 together with the soft Pomeron of hadronic physics with an intercept of about 1.08.

An analogous approach is that of [15] in which the hard Pomeron is modelled within the BFKL framework. A similar conclusion is reached, that for diffractive reactions on a hadronic target the purely perturbative regime is not reached until rather large values of Q^2 .

Combining the dipole formalism with the two-Pomeron approach allows predictions to be made for the $\gamma^{(*)}\gamma^{(*)}$ cross-sections [8]. An appropriate model for soft Pomeron exchange is the eikonal approach [16] to high energy scattering. It is particularly suited to incorporate the non-perturbative aspects of QCD which are treated in the Model of the Stochastic Vacuum [17, 18, 19], which approximates the infrared part of QCD by a Gaussian stochastic process in the colour field strength. The two-Pomeron approach of [12] has been adapted to the MSV model in [20] and successfully tested for the photo- and electroproduction of vector mesons, and for the proton structure function over a wide range of x and Q^2 .

With all parameters determined from hadronic scattering and deep inelastic scattering, in principle the model can then predict all the $\gamma^{(*)}\gamma^{(*)}$ cross-sections [8]. The only caveat is that the Pomeron contribution to $\sigma_{\gamma\gamma}$ is rather sensitive to the effective light quark mass m_q entering the photon wave function, varying as $\sim 1/m_q^4$.

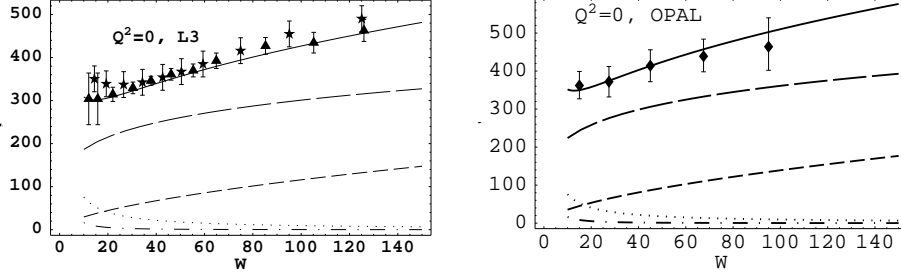


Figure 3. The total hadronic photon-photon cross-section $\sigma_{\gamma\gamma}$ (in nb) as function of W (in GeV).

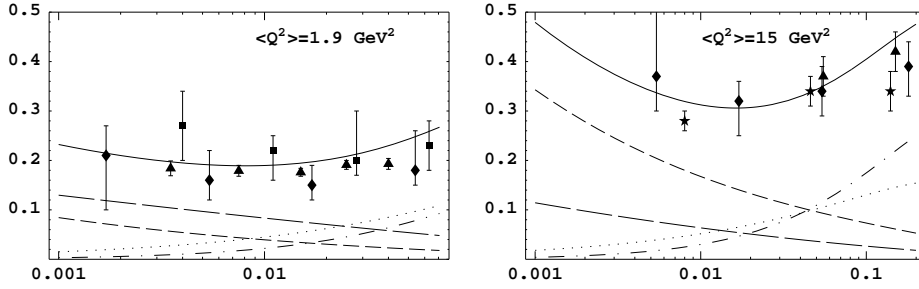


Figure 4. The photon structure function F_2^γ as function of x . a) $\langle Q^2 \rangle = 1.9 \text{ GeV}^2$, (L3: triangles, OPAL: diamonds and boxes); b) $\langle Q^2 \rangle \approx 15 \text{ GeV}^2$, (ALEPH: stars, L3: triangles, OPAL: diamonds and boxes).

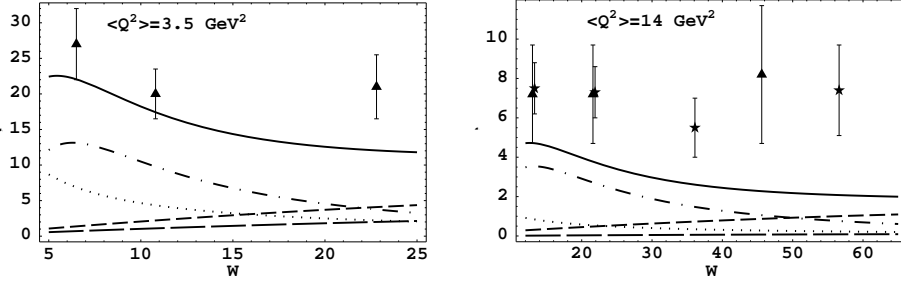


Figure 5. The virtual photon cross-section $\sigma_{\gamma^*\gamma^*}$ in nb. L3 data points are shown.

This is illustrated in Figs. 3a and b which show separately the L3 [1, 2] and OPAL [3] data and the Pomeron model with $m_q = 210 \text{ MeV}$ and 200 MeV respectively, together with the other contributions to the total cross-section. These values of m_q are within the range previously determined, and the choice does not affect the predictions away from $Q^2 = 0$. Comparison of the predictions with F_2^γ at $\langle Q^2 \rangle = 1.9$ and 15 GeV^2 are shown in Figs. 4 a and b respectively. They clearly provide a satisfactory description of the data. However comparison with $\sigma_{\gamma^*\gamma^*}$ is much less successful as is evident in Figs. 5a and b, for which $\langle Q_1^2 \rangle = \langle Q_2^2 \rangle = 3.5$ and 14 GeV^2 respectively.

The significance of these results is that a well-tried model of diffraction which successfully describes high-energy hadronic interactions, vector meson photo- and

electroproduction, deep inelastic scattering at small x , the real $\gamma\gamma$ cross-section and the structure function of the real photon fails to predict correctly the $\gamma^*\gamma^*$ cross-section even at quite modest photon virtualities. This is clearly due to the fact that, uniquely among these various processes, the $\gamma^*\gamma^*$ interaction involves two small dipoles. It emphasizes the importance of the $\gamma^*\gamma^*$ cross-section as a probe of the dynamics of the perturbative hard Pomeron.

4. $\gamma^*\gamma^*$ scattering in the BFKL formalism

The application of the BFKL formalism to $\gamma^*\gamma^*$ scattering has been considered by [21-26]. In the BFKL formalism there is a problem at LLO in setting the two mass scales on which the cross-section depends: the mass μ^2 at which the strong coupling α_s is evaluated and the mass Q_s^2 which provides the scale for the high energy logarithms.

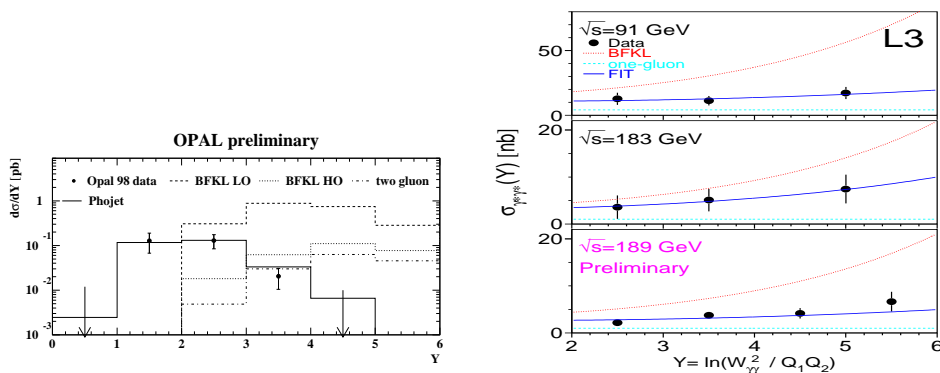


Figure 6. Cross-section for the process $e^+e^- \rightarrow e^+e^-\gamma^*\gamma^* \rightarrow e^+e^-$ hadrons as a function of $Y \approx \ln(W^2/Q_1^2 Q_2^2)$ (for exact kinematic cuts see [28] and [29]).

The result is very sensitive to these parameters, and Brodsky et al [23, 24] showed that changing $\mu^2 \rightarrow 4\mu^2$ or $Q_s^2 \rightarrow Q_s^2/4$ alters the predicted cross-section by factors of $\sim 1/4$ or ~ 4 respectively in a typical LEP experiment. An additional uncertainty is due to the correct treatment of the production of massive charm quarks.

In an attempt to overcome the scale problem, Boonekamp et al [25] take a phenomenological approach to estimate the NNLO effects, making use of a fit [27] to the proton structure function using the QCD dipole picture of BFKL dynamics. This reduces both the size of the BFKL cross-section and its energy dependence. Fig. 6 shows the preliminary OPAL measurement of the double-tag e^+e^- cross-section in the range $Q_1^2 \approx Q_2^2 \approx 5 - 25 \text{ GeV}^2$ [28] compared to the LO BFKL calculation and to the HO model of Boonekamp et al. [25]. The cross-section predicted by PHOJET [5] is also shown. The L3 collaboration has extracted the $\gamma^*\gamma^*$ cross-section using the photon flux for transverse photons (Fig. 6) [29]. The QPM part (box diagram) has been subtracted (the unsubtracted cross-section is shown in Fig. 5). The L3 data is compared to a LO BFKL prediction and to the two-gluon exchange cross-section (here called one-gluon) based on Ref. [24] and to a fit of the hard Pomeron intercept. A calculation [26] of subleading corrections to the BFKL equation shows that these are significant at LEP energies, and with the inclusion of the soft Pomeron a reasonable description of the L3 data is obtained.

Both experiments observe that the cross-section predicted by PHOJET, which does not contain BFKL effects, is consistent with the data within the large experimental errors, whereas LO BFKL predictions overestimate the $\gamma^*\gamma^*$ cross-section by a large factor. However, the large theoretical uncertainties discussed above need to be taken into account.

5. Conclusions

In the last year difficulties have emerged with the application of the Altarelli-Parisi equation to the evolution of the proton structure function at small x and with the BFKL equation. These are summarised in [30]. One of the questions is whether intrinsically non-perturbative contributions are involved, even at quite large Q^2 , because of the intrinsically non-perturbative target. This complication is in principle avoided in $\gamma^*\gamma^*$ reactions as both are dominated at large Q^2 by the perturbative part of the photon wave function. This may be happening at quite modest values of Q^2 , providing LEP with an excellent opportunity to clarify this question.

References

- [1] L3 Collaboration, M Acciari et al: Phys. Lett. B408 (1997) 450
- [2] L3 Collaboration, M Acciari et al: L3 Note 2400, *submitted to EPS99, Tampere, Finland*
- [3] OPAL Collaboration, G Abbiendi et al: CERN-EP/99-76, submitted to Eur. Phys. J. C
- [4] T Sjöstrand: Comp. Phys. Comm. 82 (1994) 74
- [5] R. Engel and J. Ranft: Phys. Rev. D54 (1996) 4244; R. Engel: Z. Phys. C66 (1995) 203
- [6] E Witten: Nucl. Phys. B120 (1977)189;
C T Hill and G Ross: Nucl.Phys. B148 (1979) 373
- [7] A Donnachie, H G Dosch and M Rueter: hep-ph/9810206, Phys. Rev.D (in press)
- [8] A Donnachie, H G Dosch and M Rueter: hep-ph/9908413, Eur. Phys. J.C (in press)
- [9] K Golec-Biernat and M Wüsthoff: Phys. Rev D59 (1999) 014017
- [10] J R Forshaw, G Kerley and G Shaw: Phys. Rev. D60 (1999) 074012
- [11] M McDermott, L Frankfurt, V Guzey and M Strikman, in preparation
- [12] A Donnachie and P V Landshoff: Phys.Lett.B447 (1998) 408
- [13] A Donnachie and P V Landshoff: hep-ph/9910262
- [14] A Donnachie and P V Landshoff: hep-ph/9912312
- [15] V V Anisovich, L G Dakhno, D I Melikhov, V A Nikonov and M G Ryskin: Phys.Rev. D60 (1999) 074011
- [16] O Nachtmann: Ann. Phys.209 (1991) 436
- [17] H G Dosch: Phys. Lett.B190 (1987) 555
- [18] H G Dosch and Yu A Simonov: Phys. Lett.B205(1988) 339
- [19] H G Dosch, E Ferreira and A Krämer: Phys. Rev. D50 (1994) 1992
- [20] M Rueter: hep-ph/9807448, Eur. Phys. J. C (in press)
- [21] F Hautmann: Proceedings of the XXVIII International Conference on High Energy Physics ICHEP96 (Warsaw, July 1996), eds. Z Ajduk and A K Wroblewski, World Scientific, p.705
- [22] J Bartels, A De Roeck and H Lotter: Phys. Lett. **B389** (1996) 742
- [23] S.J.Brodsky, F.Hautmann and D.E.Soper: Phys.Rev.Lett. **78** (1997) 803; Erratum ibid **79** (1997) 3544
- [24] S.J.Brodsky, F.Hautmann and D.E.Soper: Phys.Rev. **D56** (1997) 6957
- [25] M Boonekamp, A De Roeck, C Royon and S Wallon: hep-ph/9812523
- [26] J Kwiecinski and L Motyka: Phys. Lett. B462 (1999) 203
- [27] A Bialas, R Peschanski and C.Royon: Phys. Rev. **D57** (1998) 6899
H.Navelet, R.Peschanski and C.Royon: Nucl.Phys. **B534** (1998) 297
- [28] M Przybycień: proc. of PHOTON 99, ed. S. Söldner-Rembold, Nucl. Phys. Proc. Suppl., Vol 82, March 2000
- [29] L3 Collaboration, M Acciari et al: Phys. Lett. B453 (1999) 333;
P Achard: proc. of PHOTON 99, ed. S. Söldner-Rembold, Nucl. Phys. Proc. Suppl., Vol. 82, March 2000
- [30] R D Ball, P V Landshoff, these proceedings